International Journal of Science and Research (IJSR)
ISSN: 2319-7064
SJIF (2022): 7.942

Exploring some Aliphatic Dicarboxylate Iron based MOFs on the Fenton and Photo-Fenton like Degradation of Methylene Blue

H. Bhasin[1], P. Kashyap[2], Dr. D. Mishra[3]

Institutional Address: Department of Chemistry, School of Sciences- Gujarat University, India
Tel : + 91 9408756544, Email: *hinali.bhasin02[at]gmail.com*

Abstract: ***Four iso-structural Fe-MOFs based on aliphatic di-carboxylate linkers were synthesized to employ as peroxidase like catalyst for fenton and photo-fenton like degradation of methylene blue (MB) in water. The synthesized MOFs were characterized using SEM, FTIR, PXRD and BET. The reaction parameters that affect MB degradation were investigated such as pH of the solution, concentration of catalyst and H2O2 concentration, linker chain effect, and temperature. The results exhibit a wide range of working pH (3-11), temperature tolerance and good recyclability for MB removal in wide pH range. Scavenger insertion and fluorescent probe (UV_VIS) results suggest the involvement of hydroxyl radicals in MB degradation. These findings provide a new insight into the application of highly efficient synthesized Fe-MOFs based fenton and photo-fenton like heterogeneous catalysts and linker chain effect for their enhanced application.***

Keywords: Advanced Oxidation Processes (AOPs), Methylene Blue degradation, Metal-Organic Frameworks, fenton/photo-fenton reactions, waste-water treatment.

1. Introduction

Amongst the myriad environmental problems hovering in the world, water pollution has become one of the most hazardous source to the living beings.[1, 2] With the cumulative development of large scale textile, printing and paper-making industries, massive amount of synthetic organic contaminants such as dyes, pharmaceuticals and personal care products (PPCPs), and pesticides are being released daily into different type of wastewater bodies which eventually arrive into natural water bodies. It is estimated that about 5-10% of commercial dyes will flow into the environment along with the discharge of industrial wastewater.[3, 4] It is well known that the main characteristics of these compounds are darker color, high stability to sunlight irradiation and resistance to microbial attack.[5-7] These compounds are majorly known as persistent organic pollutants (POPs) as they also possess the ability to cause damage to living aquatic organisms as well as human beings.[8, 9] These wastewaters, if not treated judiciously may pose a significant threat to the ecosystem and human health. Thus, it is imperative to develop an effective method for eliminating these compounds from environment.

At present times, the main methods of treating dye wastewater are adsorption, photocatalysis, membrane separation, biochemical technology, advanced oxidation processes (AOPs) etc.[10-13] Amongst these, AOPs are considered as a promising method for the remediation of such wastewater. AOPs have been demonstrated to achieve good results for the elimination of organic pollutants from wastewater with very short treatment times. One of the several efficient AOPs is the use of Fenton and Photo-Fenton reactions. Fenton and Photo-Fenton reactions typically use Fe-based catalyst that react with H_2O_2 to generate hydroxylradicals (OH), resulting in the oxidation of various pollutants into non-toxic byproducts.[14-17] Small molecule, iron-based homogeneous catalysts such as co-ordination complexes or Fe-salts were originally investigated and reported as effective catalysts for these processes in mid-late 1900s; however, they displayed severe drawbacks such as high pH dependence, specifically with homogeneous catalysts typically yielding ferric hydroxide sludge at pH values above 4.0.[18-20] Therefore, heterogeneous fenton processes using solid catalysts such as iron oxide nanoparticles were investigated as a potential alternative.[21-23] However, these nanoparticle based technologies have displayed several drawbacks such as high metal leaching, nanoparticle aggregation and high recovery cost.

Metal Organic Frameworks (MOFs) offer new opportunities for the development of fenton type catalysts due to their chemical tenability, well-defined structures, large pore volumes and high surface areas.[24-26] Compared with traditional porous solids, such as zeolites, activated carbon, mesosporous silicas, MOFs allow for the precise design of their framework structures and the tailoring of their pore environments at the molecular level. Herein, we report the removal of Methylene Blue (MB) by synthesized Fe-based MOFs (Fe-MIL-88a-Pima, Fe-MIL-88a-Suba, Fe-MIL-88a-Azla and Fe-MIL-88a-Seba). The aim of this work was to evaluate the potential of employing Fe-based MOFs as peroxidase mimic catalysts in Fenton and Photo-Fenton-like reactions for removal of organic dyes from the wastewater.[27-29]

2. Materials and Methods

Materials & Reagents

Ferric (III) Nitrate nonahydrate, pimelic acid, suberic acid, azelaic acid, sebacic acid, NaOH, DMF, ethanol, Methylene Blue, Hydrogen Peroxide (H_2O_2) (30% w/w) etc were purchased from sigma Aldrich. All chemical reagents were of analytical grade and directly employed without any

further purification. During the experiment, deionized water was used to prepare all the aqueous solutions.

Catalyst Preparation

The Solvothermal method is a typical method for synthesizing Metal-Organic Frameworks that was procured to prepare Fe-MOFs utilized for the degradation of MB. Fe-MOFs namely, Fe-MIL-88a-Pima, Fe-MIL-88a-Suba, Fe-MIL-88a-Azla and Fe-MIL-88a-Seba were synthesized according to the literature.[27, 30, 31] In a typical experiment, Ferric Nitrate Nonahydrate (1.0eq) was dissolved in DMF (15ml), simultaneously the respective organic linkers such as Pimelic acid, Suberic acid, Azelaic acid and Sebacic Acid shown in the **Error! Reference source not found.** was dissolved in another set of DMF solvent. Then, the two respective solutions were mixed and stirred for 10 minutes to obtain homogeneous suspension. After that the suspension was transferred into a 100ml Teflon-lined stainless-steel autoclave. Then, the autoclave was sealed and heated at 110°C for 48-56 hours consecutively. Subsequently, the autoclave was cooled to room temperature in natural conditions. The obtained suspension was centrifuged, and brown-red solids of the respective Fe-MOFs were separated from the suspension. These solid samples were washed with water and then with ethanol to activate the samples. Finally, solid samples were dried under vacuum at 60°C overnight. After cooling to room temperature, the solid catalysts were ground to the desired powders and used in for further experiments.

Catalyst Characterization

All the four Fe-MOFs were characterized using Powder X-ray diffraction (PXRD), Thermal gravimetric analysis (TGA), Fourier transform infrared (FTIR) spectrophotometer, N_2 sorption measurements and FE-SEM. UV−vis spectroscopy measurements for the dye adsorption and degradation were also performed.

Methylene Blue Oxidation Test

Adsorption Experiments

The selected MOF adsorbents (90 mg) were used. (No further drying or activating was performed prior to the starting experiments). The adsorbent was put into a 250 ml RBF along with 150 ml of 25 mg/L dye solution. The RBF was stirred using a magnetic stir plate at approximately 580 rpm and samples were taken at various time intervals. For each specific time interval, 2 mL of solution was removed using a 2 mL syringe and filtered through a 0.22 µm syringe filter and then a UV-Vis spectrum was obtained to determine the concentration of the MB in solution.

Catalytic Degradation Experiments

Catalytic degradation experiments were performed at a constant temperature at 40°C (using a water bath) in a 250 ml RBF that was stirred using a magnetic stir plate approximately at 400 rpm with samples removed at regular time intervals. In a typical experiment, 90 mg of the catalyst was used along with 150 mL of 25 mg/L dye solution of MB and 1 mL of H_2O_2 30% w/w.For each sample, 2 mL of solution was removed using a 2 mL syringe and filtered through 0.22µm syringe filter and then a UV-Vis spectrum was obtained to determine the concentration of MB in solution. All the experiments were performed in a dark environment for the fenton and a full wavelength halogen lamp was used as the light source for the photo-fenton reactions. During the reactions, the H_2O_2 was added, and the light source was turned on at the zero time point, with the MOF being added to the solution starting at the -60min time point.

3. Results and Discussion

Catalysts Characteristics

The x-ray diffraction patterns of all the Fe-MOFs i.e. MIL-88a-Fe-Pima, MIL-88a-Fe-Suba, MIL-88a-Fe-Azla, & MIL-88a-Fe-Seba respectively, are shown in the Figure 1. It can be deduced that the XRD intensities of all the four samples were different but the strong peak position almost approached at 2θ = 8°, 10.5°, 13° respectively, which indicated that the phase type was basically identical and resonated with MIL-88a but existed differences on its content.[32] This can also be revealed by SEM analysis (**Error! Reference source not found.**). The results proved again that the difference in the length of organic linkers for MIL-88a were influential and played an important role for XRD patterns and crystallinity of the samples. The XRD patterns of the synthesized Fe-MOFs exhibited a great agreement with the previously reported MIL-88a and other Fe based MOFs, so it could be thus considered that these four Fe-MOFs in the present work were synthesized successfully.

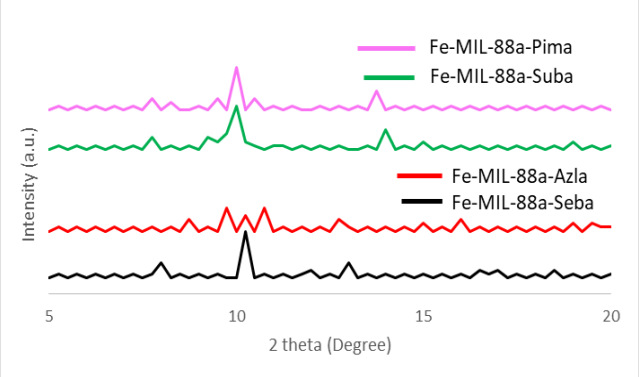

Figure 1: PXRD of All Fe-MOFs

Moreover, the structure that we examined by IR-spectra shown in Figure 2a were collected between 4000 cm^{-1} and 500 cm^{-1}. The spectrum of Fe-MIL-88a-Pima featured a broad adsorption feature between 3500-2700 cm^{-1} caused by (OH) stretching from the water molecules in the complex; additional bands at: υ_{max}/cm^{-1}; 1570 and 1523 (υ_{as} CO_2^-); 1469 and 1443 (υ_s CO_2^-); 1412 and 1396 (C-O); 1335 (CH_2); 1230 and 1215 (C-O); 1145 and 1042 (C-C) and 937, 864, 798, 741, 698, 663, 582, 555 and 532 (metal-oxygen bonds and C-H). In similar fashion, Fe-MIL-88a-Suba, Fe-MIL-88a-Azla and Fe-MIL-88a-Seba exhibited a range of significant absorption bands which were consistent with carboxylate groups and are visible in all spectra, such as the asymmetric stretch around 1600 cm^{-1} and a symmetric stretch just below 1500 cm^{-1}. Moreover, when the frequency splitting between these bands of the asymmetric and symmetric carboxylate stretching modes occurs in the range of δ = 50-150 cm^{-1}, it corresponds to bi-dentate interaction

between acid group and the cation, whereas for a bridging complexing state and the uni-dentate complex, the range falls under δ = 130-200 cm^{-1} and δ > 200 cm^{-1}, respectively. Based on these guidelines and the interactions between the linear di-carboxylates and cation systems seemed mainly to be bi-dentate type. However, for Fe-MIL-88a-Azla and Fe-MIL-88a-Seba, both bi-dentate and a bridging type of complex was observed.

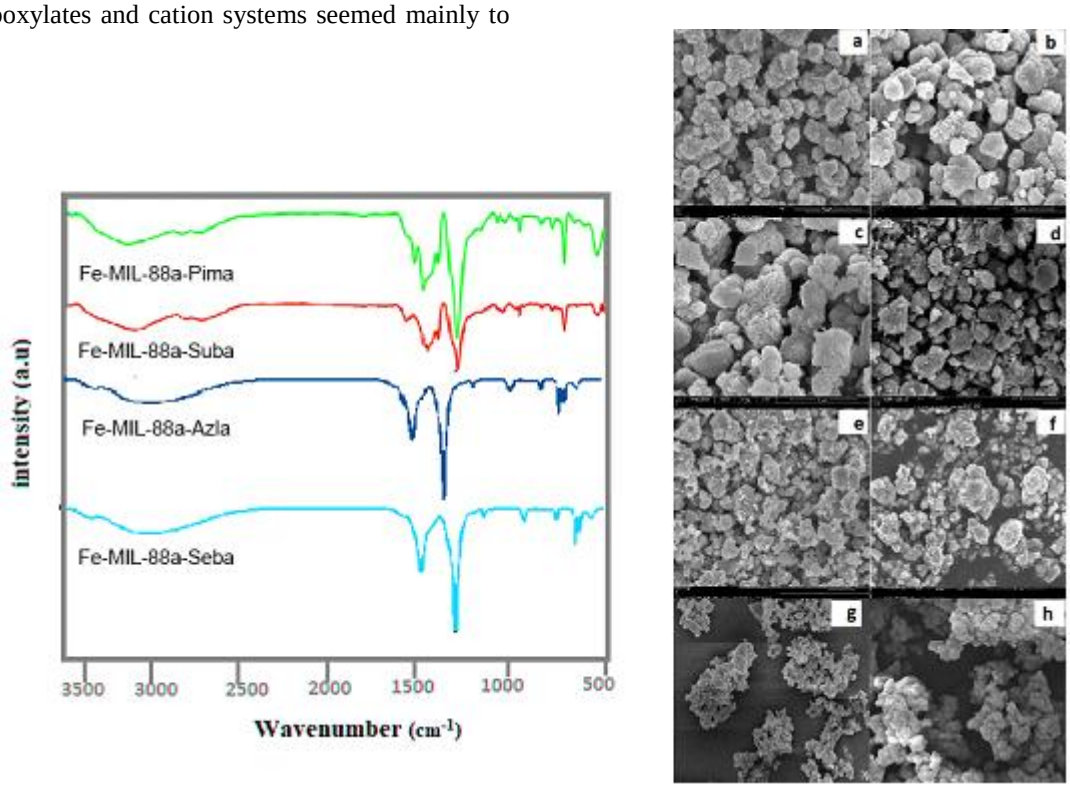

Figure 2: a) IR of Fe-MOFs b) FE-SEM images of Fe-MOFs

The morphology of Fe-MOFs was examined by SEM as shown in the Figure 2b. The samples present a standard form as colloidal spheres like morphology from a single sample scanning electron microscopy. We can observe that the crystal size grew little over the time with increase in the surface area, while the morphology of the synthesized Fe-MOFs remained unchanged. It was observed that numbers of Fe-MOFs were in growth stage and the crystal size were small and in the range of 5µm to 10µm, however the full grown stage on the whole field vision was observed when the length of the organic linkers increased. It was obvious that not only the size of the samples became larger with the increase in length of aliphatic dicarboxylate linkers, but also the overlapping and porous surfaces of the samples increased. Higher surface area and overlapping of the surfaces can be achieved while gradually increasing the length of the aliphatic linkers.

The results shown in Figure 3a exhibits N_2 sorption/desorption isotherms of Fe-MIL-88a-Pima which was a combination of the type II and III sorption isotherms. A similar pattern for the adsorption and desorption isotherms were observed by the rest of the synthesized Fe-MOFs i.e. Fe-MIL-88a-Suba, Fe-MIL-88a-Azla and Fe-MIL-88a-Seba. The results of BET surface area and pore volume of all synthesized Fe-MOFs produced were displayed in

Table ***1***. BJH adsorption suggests that pores within Fe-MOFs were mesoporous with a dominant range from 5 to 90 nm and the maximum pores present were in the range of 16 ~ 23 nm.

The thermal stability of the Fe-MOFs were analyzed through TGA and shown in the Figure 3c indicates that the as synthesized Fe-MOFs loses significant amount of weight in two regions on heating. The first of these is between 65℃ and 110℃ where 20-25% of initial weight is lost which can be consistent with the loss of water i.e., both lattice and co-ordinated from the structure. In addition to this, weight loss is consistent with the decomposition of the framework to produce Fe_2O_3 which occurs between 270℃ and 350℃ leading to final weight of 34%.

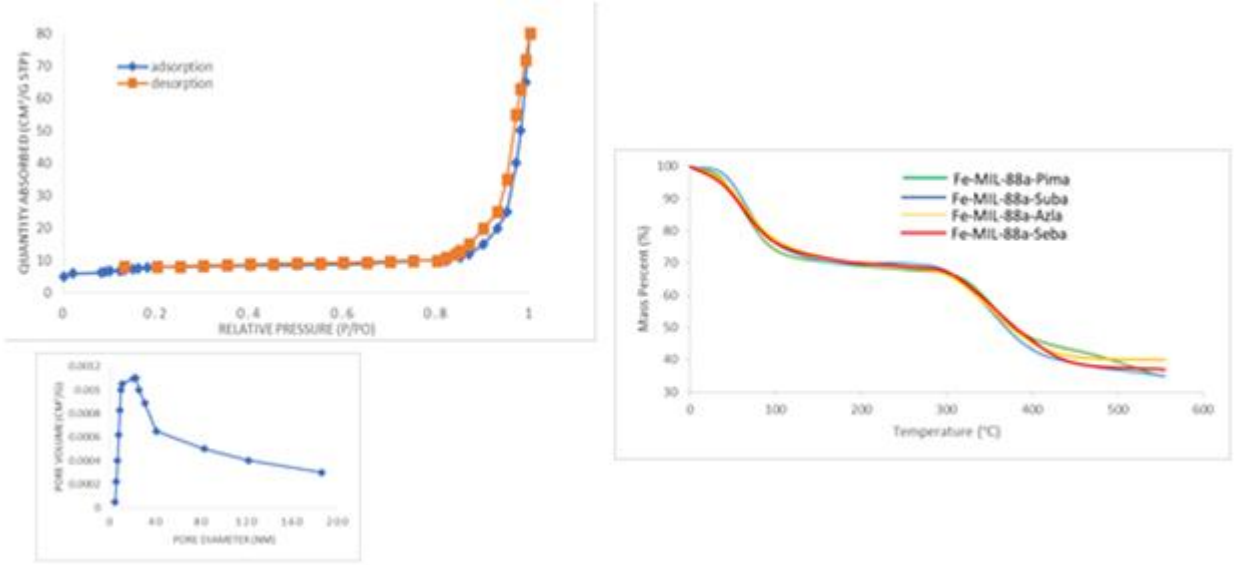

Figure 3: a) N2 Adsorption Isotherm of Fe-MIL-88a-Pima b) Pore volume diameter of Fe-MIL-88a-Pima c) TGA graphs of Fe-MOFs

Table 1: BET Surface and pore volume of all the Fe-MOFs

Increasing Linker Length	Fe-MOFs	S_{BET} (m^2/g)	T-plot micro-volume (cm^3/g x 10^{-2})	Degradation rate of MB (%)
	Fe-MIL-88a-Seba	59.61	1.24	97.3%
	Fe-MIL-88a-Azla	47.38	1.11	94.15%
	Fe-MIL-88a-Suba	33.49	0.99	89.5%
	Fe-MIL-88a-Pima	24.78	0.90	86.66%

Optimization study of the experimental conditions for fenton and photo-fenton like degradation of MB

To evaluate each sample's activity for the removal and degradation of toxic organic compounds (TOCs) from the simulated aqueous solution as well as correlate the TOC removal efficiency with the increasing surface area of the Fe-MOFs due to the cumulative length of organic linkers used, the samples were evaluated based on three criteria; dye adsorption, dye degradation using fenton reaction conditions and dye degradation using photo-fenton reaction conditions. Methylene Blue was selected as a model TOC to be used in this study because its concentration could easily and accurately be determined using UV-Vis spectroscopy. Firstly, each sample was examined for only its dye adsorption performance (no H_2O_2 or light) (Figure 4a shows all the samples displayed similar dye adsorption properties). For instance, Fe-MIL-88a-Seba displayed a dye adsorption profile in which approximately 23% of MB was removed from the 25.0 mg/L (ppm) solution after approximately 140 mins. The adsorption efficiency remains unchanged until the experiment was terminated till 720 mins. Rest other three Fe-MOFs such as Fe-MIL-88a-Pima, Fe-MIL-88a-Suba and Fe-MIL-88a-Azla also exposed a minimal adsorption profile ranging from 15-18%. This adsorption profiles of Fe-MOFs can be attributed to the strong adsorption of the dye within the micropores of the MOF crystals. Amongst the Fe-MOFs, a significant adsorption profile was exhibited by Fe-MIL-88a-Seba due to comparative higher surface area of the increasing pores, overlapping and crystal size.

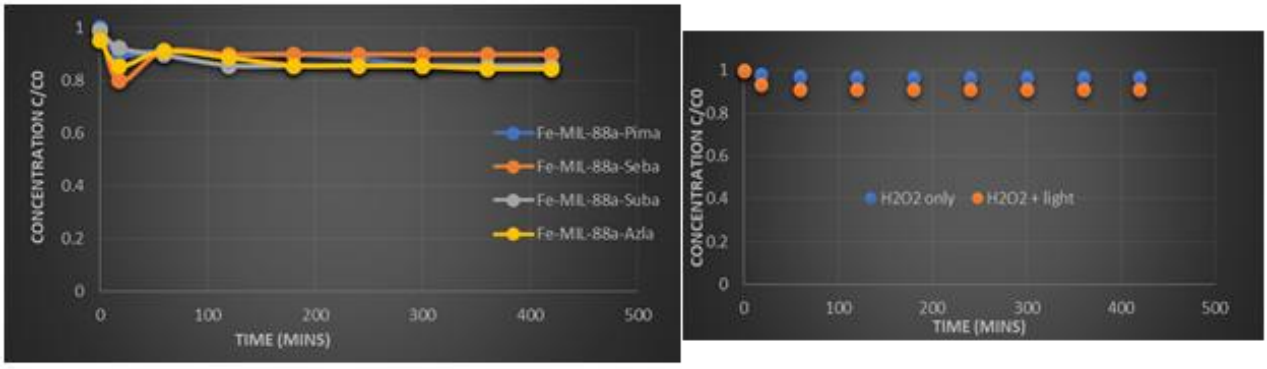

Figure 4: a) Blind Experiment with Fe-MOFs and Dye b) Blind Experiment with Light/H2O2 and dye

Next, the samples were examined as catalysts for their fenton and photo-fenton reactions, specifically for the degradation of MB taken as a TOC model. Numerous publications over the years have explored that Iron is a vital component that acts as a catalyst in oxidation of waste-water contaminants in presence of H_2O_2.[19, 33] Conventionally, this process occurs when Iron (II) is oxidized by H_2O_2 to Iron (III) forming a hydroxyl radical and a hydroxide ion. Then, oxidized Iron (III) is reduced back to Iron (II) by another molecule of hydrogen peroxide which forms hydrogen

peroxyl radical and a proton. This net effect is a disproportionation of H_2O_2 that creates two different oxygen radical species with water as a by-product. In addition to this, free radicals are generated passively by this process that engage in secondary reactions such as non-selective oxidation of organic pollutants. Besides this, in photo-fenton reactions, a light source such as halogen lamp is used which assists the radical generation process.[34, 35]

As shown in the Figure 5a, results revealed that Fe-MIL-88a-Pima, Fe-MIL-88a-Suba, Fe-MIL-88a-Azla and Fe-MIL-88a-Seba exhibits a decent performance for the degradation of MB under fenton conditions by removing nearly 85-88% of MB after 150 mins and when exposed to photo-fenton reaction conditions, all the four Fe-MOFs significantly displayed a better performance achieving 96-98% MB degradation after 90 mins which is presented in the Figure 5b. In addition to this, the results shows that the catalytic degradation efficiency of Fe-MOFs is significantly improved during photo-fenton reactions than the fenton conditions. Moreover, by the incorporation of longer linker length, the surface area increases drastically which in turn increases the fenton and photo-fenton catalytic activity of the Fe-MOFs, for instance, Fe-MIL-88a-Seba exhibited a substantial degradation efficiency than Fe-MIL-88a-Pima due to larger surface area as well as crystal growth. The optimization controlled experiments were then carried out for Fe-MIL-88a-Seba and the parameters affecting the degradation efficiency of the Fe-MIL-88a-Seba has been further discussed.Conversely and conclusively, all the four synthesized Fe-MOFs displayed a remarkable degradation efficiency against MB. Next, to verify that the catalytic degradation of MB was due to the presence of the MOF in conjugation with H_2O_2 or the light source and not the H_2O_2 or the light source alone, two control experiments were performed in the absence of the MOF samples. The first was the same degradation experiment performed with only H_2O_2 and the second was performed using H_2O_2 and the halogen light source. It should be noted that the MOF sample was omitted from both experiments. As shown in the Figure 4b, both experiments yielded little to no dye degradation. This confirmed that the MOF which acts as the catalyst, is responsible for the catalytic process of the radical generation and dye adsorption.

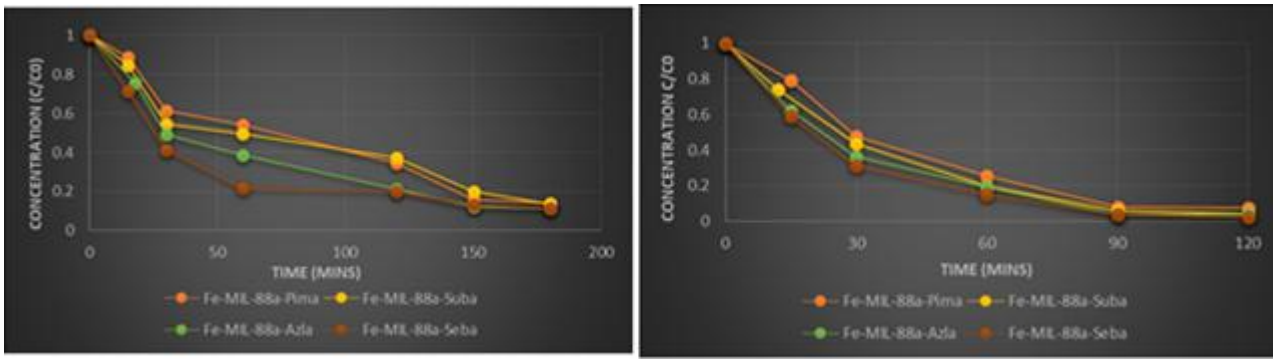

Figure 5: a) Fenton Reaction Degradation by Fe-MOFs b) Photo-Fenton Reaction Degradation by Fe-MOFs

Effect of Temperature

The temperature is an important parameter which is directly related to the generation of ·OH in fenton and photo-fenton like degradation processes. The effect of temperature on the degradation of MB (shown in the**Error! Reference source not found.**). It was found that the MB conversion and TOC removal increased with the increase of temperature from 30 ℃ to 70 ℃. The oxidation rate was also accelerated. This is since the generation of hydroxyl radicals by H_2O_2 (equation 1) is much easier and faster at higher temperatures and as a result oxidation of organics is accelerated. On the other hand, the active sites of the catalyst were not only located on the external surface but also a large portion of the active sites existed in the inner pore surface. The increase in the temperature contributed to the diffusion of H_2O_2, MB and the intermediates of the degradation process into the inner pore surface of the Fe-MOFs. Therefore, higher temperature was beneficial for the degradation of MB. As shown in the Figure 6a, for Fe-MIL-88a-Seba, when the reaction temperature was at 60℃, the MB removal efficiency was nearly 85% after 60 minutes and for the temperature of 70℃, MB removal efficiency was nearly 70% which was lower than at 60 ℃ after reaction for 90 mins. This could be attributed to the MB being easily oxidized into intermediates and which further blocks the active sites by getting trapped in the pores, hence were difficult to be mineralized. In the process of the oxidation of the intermediates, the thermal decomposition of H_2O_2 (equation 2) was serious which resulted in low utilization of H_2O_2. Therefore, too high temperature did not improve the degradation performance. Furthermore, it not only resulted in high energy consumption but also led to a waste of resources. Similar aspects were observed for the rest of the synthesized Fe-MOFs Considering all aspects including energy consumption, resource saving and the final degradation effect, 40 ℃ was considered the best temperature for the catalytic oxidation of MB by Fe-MOFs with H_2O_2 as the oxidant.

$$H_2O_2 \longrightarrow HO^{\bullet} + HO^{\bullet} \quad (1)$$

$$H_2O_2 \longrightarrow H_2O + O_2 \quad (2)$$

Effect of H_2O_2 dosage

The generation of hydroxyl radicals closely depends on the dosage of H_2O_2. In view of the added H_2O_2 not being fully utilized, more than the stoichiometric ratio of H_2O_2 is needed in most cases. With the increase of the concentration of H_2O_2 from 0.1mL to 1.5mL, the MB conversion and TOC removal showed a consistent trend. As the H_2O_2 dosage was increased from 0.1mL to 1.5mL, an increased tendency of MB conversion and TOC removal was observed with the

MB removal rising from 52.8% to 89% after 60 minutes for Fe-MIL-88a-Seba. This could be explained as the higher dosage of H_2O_2 promoted the generation of more hydroxyl radicals to oxidize MB. When the initial dosage of H_2O_2 was increased upto (1.5mL), the degradation efficiency presented a downward trend which was caused by two aspects. Firstly, it was mainly ascribed to the scavenging effect as shown by equation 3 and equation 4. A good deal of hydroxyl radicals reacted with the residual H_2O_2 producing $HO\cdot_2$ (equation 3), which has worse oxidizability than ·OH and was not beneficial for the oxidation of organics. Furthermore, the generated $HO\cdot_2$ could continue to consume ·OH to form oxygen gas (equation 4) giving rise to a severe loss of H_2O_2.

$$H_2O_2 + HO^{\cdot} \longrightarrow HO_2^{\cdot} + H_2O \quad (3)$$

$$HO_2^{\cdot} + HO^{\cdot} \longrightarrow H_2O + O_2 \quad (4)$$

In addition, excess H_2O_2 competes with the organics leading to less organics diffusing into the interior pores of the catalysts. Thus, a large number of hydroxyl radicals generated in the pores were not utilized resulting in a low MB degradation efficiency. Therefore, to get a better degradation effect, the dose of H_2O_2 should be strictly controlled.

For each batch oxidation test, 0.5 mL of H_2O_2 was identified as the optimal value for peroxidase degradation of MB (150 mL 25 mg L^{-1} MB) by Fe-MOFs.

Effect of Catalyst Dosage

In Advanced oxidation processes (AOPs), catalyst dose is an extremely important factor for the catalytic decomposition of H_2O_2 to form strongly oxidizing hydroxyl radicals. The effect of catalyst dose on the catalytic degradation of simulated MB wastewater plays an important role and hence while performing the optimization experiments, it was concluded that MB conversion and removal efficiency were strongly linked with catalyst dose. When the catalyst dose was increased from 90 mg to 200 mg, the MB degradation efficiency decreased from 98-94% to 86-83% for all the Fe-MOFs. It was concluded that more catalyst contributed to the thermal decomposition of H_2O_2 to generate water and oxygen gas (equation 2) resulting in less H_2O_2 to participate in the mineralization of MB.

$$HO^{\cdot} + \text{organics} \longrightarrow \text{intermediates} + CO_2 + H_2O \quad (5)$$

$$CO_2 + H_2O \rightleftharpoons H_2CO_3 \quad (6)$$

$$H_2CO_3 \rightleftharpoons HCO_3^{-} + H^{+} \quad (7)$$

$$HO^{\cdot} + HCO_3^{-} \longrightarrow OH^{-} + HCO_3^{\cdot} \quad (8)$$

Initially, a higher catalyst dose promoted the generation of a vast amount of hydroxyl radicals (equation 1) in a shorter time and the higher concentration of hydroxyl radicals made these equilibrium equations to shift towards right but since the nonselective oxidation shown in equation 8, less hydroxyl radicals were left to mineralize MB. Hence, MB degradation efficiency decreased when too much catalyst was employed.[36] When the catalyst dose was decreased from 90 mg to 50 mg, the MB removal efficiency decreased by 23% after 60 minutes. This was because when the catalyst concentration decreased, the number of active sites available for the catalytic production of hydroxyl radicals generated by H_2O_2 declining at the same time and the conversion efficiency dropped. Therefore, adding the optimum amount of catalyst not only economized the resources but also improved the degradation efficiency. Therefore, 90 mg Fe-MOFs were applied for further experiments with other conditions kept constant.

Effect of the pH

The initial pH of the effluents also played a critical role in the AOPs of organic compounds. In this study, the initial pH of the simulated phenol wastewater was adjusted by diluted nitric acid and ammonia solution ranging from 2.0 to 10.0 to evaluate the influence of pH on the degradation process is clearly presented in Figure 6b. It was obvious that the catalytic performance of Fe-MOFs closely depended on the initial pH of the MB solution. The optimal degradation efficiency was obtained at the pH 3.5 and the MB degradation efficiency reached 96% after 90 minutes for Fe-MIL-88a-Seba. Extremely lower or higher pH were not beneficial to the degradation of MB especially when the pH of the MB was too low or too high, the degradation of MB was severely impeded. This could be interpreted as that, in the basic conditions, H_2O_2 was more inclined to break down into H_2O and O_2 at high speed (equation 2) instead of generating hydroxyl radicals accounting for only a tiny portion of the H_2O_2 participating in the mineralization of organics. This not only resulted in a waste of resources, but also weakened the degradation effect. In consequence, alkaline conditions were not suitable for the degradation of simulated MB wastewater by the as-synthesized Fe-MOFs. It can attribute to the Fe hydroxide formation. For acidic environment, especially for heavily acidic conditions, the poor degradation efficiency could be attributed to the leaching of Fe^{3+} from the catalyst. The loss of Fe from the catalyst was equivalent to the reduction of the active sites which were directly related to the catalytic activity of the Fe-MOFs. In other words, strongly acidic conditions resulted in the deactivation of the catalyst to a certain degree leading to the poor mineralization of MB. Thus, slightly acidic pH conditions were more suitable for the catalytic oxidation of MB wastewater. Considering the facts, 25 mg L^{-1} of MB solution was taken, and subsequent experiments were conducted at the pH 3.5.

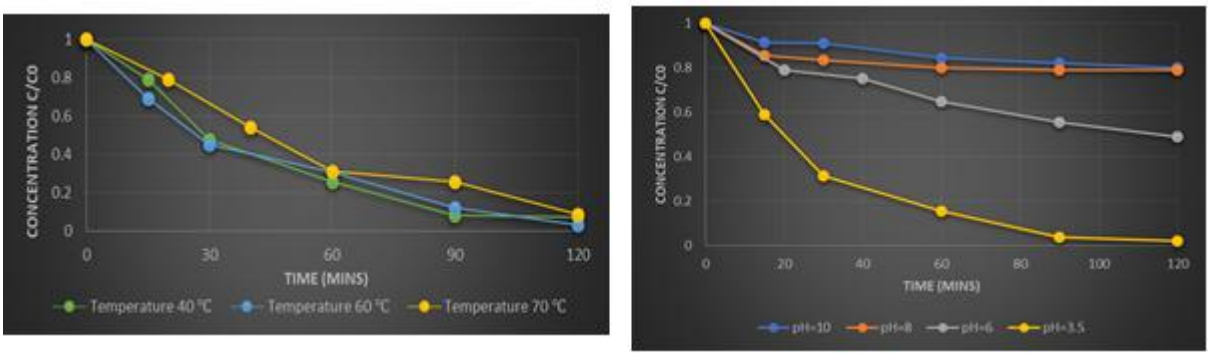

Figure 6: a) Effect of Temperature b) Effect of pH

Degradation Catalytic Mechanism and Reusability of Fe-MOFs

In general, the degradation process proceeded by the hydroxyl radical mechanism when Fe-based catalysts were applied for the catalytic wet peroxide oxidation of organic effluents. However, it was unclear whether the catalytic degradation mechanism here was the same as the other reported Fe-based catalysts for the catalytic oxidation of MB by Fe-MOFs. Tert-Butanol, as a kind of common hydroxyl radical scavenger was employed for investigating the mechanism. When tert-butanol was added into the reaction system, no change in the color was observed throughout the experimental process. It seemed that the MB was not degraded at all. Then, the MB conversion efficiency and TOC removal efficiency were measured, anda noticeable observation was made that the conversion of MB was less than 5%, indicating the negligible degradation of MB. This negligible degradation of MB was raised by the adsorption via Fe-MOFs, while the added tert-butanol severely inhibited the catalytic degradation of MB by consuming the hydroxyl radicals generated by H_2O_2. Hence, it was concluded that the catalytic oxidation of MB by Fe-MOFs did follow the hydroxyl radical mechanism which was in accordance with the other reported Fe-based catalysts.

From the industrial application viewpoint, the key role is the recyclability of the catalyst. To evaluate the long-term recyclability of the Fe-MOFs, a recycling study of three runs was conducted for the catalytic oxidation of MB. In the recycling study the degradation process was controlled under the optimum conditions. The MB conversion efficiency for Fe-MIL-88a-Seba could still reach nearly 94% after reaction for 1hr except that the conversion rate showed a downward trend compared with the first run (Figure 7). However, the final TOC removal efficiency decreased in a noticeable manner with each run and a similar trend was observed for the rest of the synthesized Fe-MOFs. A consistent collapse of the framework part with each run, might have resulted in the declining trend. After three runs, more than80% TOC removal efficiency for all the synthesized Fe-MOFs was still achieved indicting the favorable reusability of these Fe-MOFs. Thus, the synthesized Fe-MOFs was indeed satisfactory heterogeneous catalyst for the wastewater treatment.

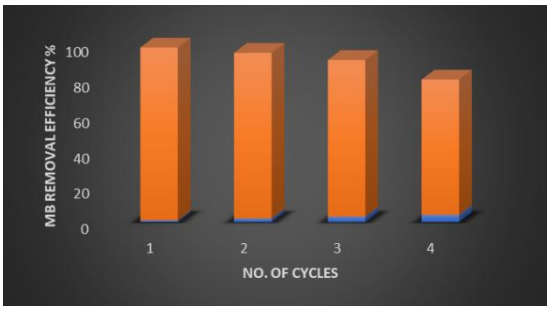

Figure 7: Recyclability of Fe-MOFs

4. Conclusion

This work describes the peroxidase like catalytic degradation of simulated methylene blue wastewater by four different Fe-MOFs namely Fe-MIL-88a-Pima, Fe-MIL-88a-Suba, Fe-MIL-88a-Azla and Fe-MIL-88a-Seba. Under similar conditions, the Fe-MIL-88a-Seba exhibited a higher catalytic activity than the other three Fe-MOFs, which was mainly ascribed to the higher surface area possessed by the Fe-MIL-88a-Seba leading to easy entrance into the pores of organics. The parameters affecting the catalytic oxidation of methylene blue were also investigated and the optimal degradation conditions were obtained. Satisfactory degradation performance was achieved with methylene blue removal of 97%. After being reused thrice, the Fe-MIL-88a-Seba still retained satisfactory catalytic activity. The catalytic oxidation of methylene blue was closely dependent on the highly active hydroxyl radicals. The synthesized Fe-MOFs possessed a strong ability to adapt to the simulated methylene blue wastewater of different concentrations. Therefore, Fe-MOFs could be promising heterogeneous catalysts for peroxidase degradation of organic effluents.

References

[1] F. Owa, Mediterranean journal of social sciences,4(8): p. 65-65 (2013).
[2] P. Goel, New Age International, (2006).
[3] B. Lellis, et al., Biotechnology Research and Innovation, 3(2): p. 275-290, (2019).
[4] F. Owa, International Letters of Natural Sciences, 3 (2014.).
[5] A. Gürses, et al., *Dyes and Pigments*. Springer. p. 13-29(2016)
[6] S. El Harfi and A. El Harfi, Applied Journal of Environmental Engineering Science,**3**(3)311-320 (2017)

[7] M.A. Hassaan, A. El Nemr, and A. Hassaan, American Journal of Environmental Science and Engineering, **1**(3): p. 64-67 (2017).
[8] H. Bhasin, and D. Mishra, Comments on Inorganic Chemistry, **41**(5): p. 267-315 (2021).
[9] T. Robinson, et al., Bioresource technology, **77**(3): p. 247-255 (2001).
[10] H. Anwer, et al., Nano Research, **12**(5): p. 955-972 (2019).
[11] S. Varjani, et al., Bioresource Technology, **314**: p. 123728 (2020).
[12] P.V. Nidheesh, R. Gandhimathi, and S.T. Ramesh, Environmental Science and Pollution Research, **20**(4): p. 2099-2132(2013).
[13] S.Sarkar,et al., Water Conservation Science and Engineering, **2**(4): p. 121-131 (2017).
[14] M.-h. Zhang, et al., Science of the Total Environment, **670**: p. 110-121 (2019).
[15] P.Shandilya, P. Raizada, and P. Singh, *Water Pollution and Remediation: Photocatalysis*. Springer. p. 119-146 (2021).
[16] B. Jain, et al., Environmental Chemistry Letters, **16**(3): p. 947-967 (2018).
[17] N. Thomas, D.D. Dionysiou, and S.C. Pillai, Journal of Hazardous Materials, **404**: p. 124082 (2021).
[18] S. Matavos-Aramyan, and M. Moussavi, Int. J. Environ. Sci. Nat. Resour,**2**(4): p. 1-18 (2017).
[19] J. He, et al., Journal of environmental sciences,**39**: p. 97-109 (2016).
[20] F. Rezaei, and D. Vione, Molecules,**23**(12): p. 3127 (2018).
[21] C. Hitam, and A. Jalil, Journal of environmental management,**258**: p. 110050 (2020).
[22] R. Saleh, and A. Taufik, Separation and Purification Technology,**210**: p. 563-573 (2019).
[23] S. R. Pouran, et al., Journal of Cleaner Production,**64**: p. 24-35 (2014).
[24] M. J. Uddin, R.E. Ampiaw, and W. Lee, Chemosphere,**284**: p. 131314 (2021).
[25] V. K. Sharma, and M. Feng, Journal of hazardous materials,**372**: p. 3-16 (2019).
[26] S. Lu, et al.,Environment International,**146**: p. 106273 (2021).
[27] J. Castells-Gil, N.M. Padial, and C. Martí-Gastaldo, New Journal of Chemistry, **42**(19): p. 16138-16143 (2018).
[28] C. Du, et al., Chemical Engineering Journal,**431**: p. 133932 (2022).
[29] S. Li, et al., *A review*. Journal of Environmental Chemical Engineering,**9**(5): p. 105967 (2021).
[30] E. Bagherzadeh, et al., CrystEngComm,**21**(3): p. 544-553 (2019).
[31] V.P. Viswanathan, et al., *on the Photocatalytic Degradation of Rhodamine B.* ChemistrySelect,**5**(25): p. 7534-7542 (2020).
[32] E. Bagherzadeh, S.M. Zebarjad, and H.R.M. Hosseini, European Journal of Inorganic Chemistry, **2018**(18): p. 1909-1915 (2018).
[33] A.D. Bokare, and W. Choi, Journal of hazardous materials,**275**: p. 121-135 (2014).
[34] U.J. Ahile, et al., Science of the Total Environment,**710**: p. 134872 (2020).
[35] S. Giannakis, et al., Applied Catalysis B: Environmental, **199**: p. 199-223 (2016).
[36] S. Zhang, et al.,Chemical Engineering Journal,**252:** p. 141-149 (2021).